Inorg. Chem. **1994**, *33*, 227–232

Chiral Discrimination in the Reduction of $[Co(edta)]^-$ by $[Co(en)_3]^{2+}$ and $[Ru(en)_3]^{2+}$. X-ray Structure of $[\Lambda\text{-}Co(en)_3][\Delta\text{-}Co(edta)]_2Cl\cdot 10H_2O$

Robert M. L. Warren, Kenneth J. Haller, Akira Tatehata, and A. Graham Lappin*

Department of Chemistry and Biochemistry, University of Notre Dame, Notre Dame, Indiana 46556

Received July 20, 1993[⊗]

The structure of the salt $[\Lambda\text{-}Co(en)_3][\Delta\text{-}Co(edta)]_2Cl\cdot 10H_2O$ has been determined by X-ray crystallography. The salt crystallizes in the orthorhombic space group $P2_12_12$ (No. 18) with $Z = 2$, $a = 21.046(3)$ Å, $b = 12.813(2)$ Å, $c = 8.158(1)$ Å, and $R = 0.035$ for 5263 reflections. The complex ions participate in a network of hydrogen bonds which is interpreted to suggest a mechanism for chiral discrimination. Outer-sphere reduction of $[Co(edta)]^-$ by $[Ru(en)_3]^{2+}$ takes place with a second-order rate constant of 6×10^3 M^{-1} s^{-1} at 25 °C and 0.10 M ionic strength. Chiral induction in the reaction results in a 2% enantiomeric excess with a $\Delta\Lambda$ preference, significantly smaller than the 10% $\Delta\Lambda$ induction found with $[Co(en)_3]^{2+}$ as reductant. This difference in chiral induction between the two reductants is ascribed to differences in chiral recognition in the assembly of electron-transfer precursor complexes.

The reduction of $[Co(edta)]^-$ (edta^{4-} = 1,2-diaminoethane-*N,N,N′,N′*-tetraacetate(4−)) by $[Co(en)_3]^{2+}$ (en = 1,2-diaminoethane) has evolved as a prototype for outer-sphere electron-transfer reactions in which chiral induction is observed.[1,2] The stereoselectivity favors the heterochiral pair or $\Delta\Lambda$ pair, with an enantiomeric excess around 10% in aqueous solution at 25 °C. Electron transfer is believed to take place through a precursor complex in which the carboxylate face of the oxidant is involved in a dominant, hydrogen-bonding interaction with amine protons from the reductant.[3,4] The stereochemical preference changes from heterochiral when the C_3 axis of the reductant is sterically hindered as in $[Co(sep)]^{2+}$ (sep = 1,3,6,8,10,13,16,19-octaazabicyclo[6.6.6]icosane) to homochiral when steric hindrance is placed perpendicular to this axis as in *lel*$_3$-$[Co(chxn)_3]^{2+}$ (chxn = *trans*-1,2-diaminocyclohexane).[3] These differences are also detected in stereoselectivity in the ion-pair interactions between $[Co(edta)]^-$ and the analogues $[Co(sep)]^{3+}$ and *lel*$_3$-$[Co(chxn)_3]^{3+}$,[5–7] leading to the suggestion that the ion pairs are good models for the electron-transfer precursor. It has also been suggested that chiral induction in the electron-transfer reaction is determined by chiral recognition in the precursor. Limited information on the orientation of the ions in the ion pairs in solution has been obtained from NMR experiments, but the model lacks structural detail.[8]

Recently, evidence was obtained to suggest that stereoselectivity is not determined solely by chiral recognition in the precursor but that other factors, less well understood, also operate.[9,10] One way to investigate this phenomenon is to examine reactions of isostructural complexes with different metal ions. Accordingly, the reduction of $[Co(edta)]^-$ by $[Ru(en)_3]^{2+}$ has been investigated and is compared with the corresponding reduction by $[Co(en)_3]^{2+}$. In addition, the X-ray and molecular structure of $[\Lambda\text{-}(+)_{589}\text{-}Co(en)_3][\Delta\text{-}(+)_{546}\text{-}Co(edta)]_2Cl\cdot 10H_2O$ is reported and comparisons with the solution structure are drawn. The relationship of this structure to the previously published structure[11] $[\Delta\text{-}Ni(en)_3][\Delta\text{-}Ni(edta)]\cdot 4H_2O$ provides some important clues about the mechanism of chiral discrimination in the electron-transfer precursor.

Experimental Details

Preparations of $Na[Co(edta)]\cdot 2H_2O$,[12] $Na[\Delta\text{-}(+)_{546}\text{-}Co(edta)]\cdot 4H_2O$ ($\epsilon_{535} = 331$ M^{-1} cm^{-1}, $\Delta\epsilon_{575} = -1.79$ M^{-1} cm^{-1}),[13,14] $[\Lambda\text{-}(+)_{589}\text{-}Co(en)_3]Cl_3\cdot H_2O$ ($\epsilon_{467} = 88$ M^{-1} cm^{-1}, $\Delta\epsilon_{485} = -1.90$ M^{-1} cm^{-1}),[15,16] $K_3[Co(ox)_3]\cdot 3.5H_2O$,[17] and $K_3[\Delta\text{-}(+)_{589}\text{-}Co(ox)_3]\cdot 3.5H_2O$ ($\epsilon_{605} = 165$ M^{-1} cm^{-1}, $\Delta\epsilon_{622} = -3.80$ M^{-1} cm^{-1})[18–20] have been described. Violet crystals of $[\Lambda\text{-}(+)_{589}\text{-}Co(en)_3][\Delta\text{-}(+)_{546}\text{-}Co(edta)]_2Cl\cdot 10H_2O$ were obtained by the addition of 0.051 g (0.12 mmol) of $Na[\Delta\text{-}(+)_{546}\text{-}Co(edta)]\cdot 4H_2O$ to a solution of 0.038 g (0.1 mmol) of $[\Lambda\text{-}(+)_{589}\text{-}Co(en)_3]Cl_3\cdot H_2O$ in 3 mL of water. Crystals suitable for X-ray analysis were grown as flat rods by diffusion of propan-2-ol into an aqueous solution of the compound. The composition of the crystals was checked by absorption, CD spectroscopy and by chromatographic separation of the components on SP-Sephadex C-25 prior to X-ray analysis. $K_3[Rh(ox)_3]\cdot 4.5H_2O$ was prepared[21] from freshly precipitated rhodium hydroxide and potassium hydrogen oxalate,[22] and resolution was achieved[20,23] using $[\Lambda\text{-}(+)_{589}\text{-}Ni(phen)_3](ClO_4)_2\cdot 3H_2O$ to give $K_3[\Lambda\text{-}(+)_{546}\text{-}Rh(ox)_3]\cdot 2H_2O$ ($\epsilon_{402} = 330$ M^{-1} cm^{-1}, $\Delta\epsilon_{400} = +2.85$ M^{-1} cm^{-1}).[24] Commercially available $[Ru(en)_3]Cl_2$ (Alfa) was purified as described.[25] $[Ru(en)_3]I_3$ was prepared by iodine oxidation of the ruthenium(II) salt[26] and resolved using K_3-

---

[⊗] Abstract published in *Advance ACS Abstracts,* December 15, 1993.

(1) Geselowitz, D. A.; Taube, H. *J. Am. Chem. Soc.* **1979**, *101*, 883–892.

(2) Lappin, A. G.; Marusak, R. A. *Coord. Chem. Rev.* **1991**, *109*, 125–180.

(3) Osvath, P.; Lappin, A. G. *Inorg. Chem.* **1987**, *26*, 195–202.

(4) Geselowitz, D. A.; Hammershøi, A.; Taube, H. *Inorg. Chem.* **1987**, *26*, 1842–1845.

(5) Sakaguchi, U.; Yamamoto, I.; Izumoto, S.; Yoneda, H. *Bull. Chem. Soc. Jpn.* **1983**, *56*, 1407–1409.

(6) Miyoshi, K.; Sakamoto, Y.; Ohguni, A.; Yoneda, H. *Bull. Chem. Soc. Jpn.* **1985**, *58*, 2239–2246.

(7) Tatehata, A.; Fujita, M.; Ando, K.; Asaba, Y. *J. Chem. Soc., Dalton Trans.* **1987**, 1977–1982.

(8) Marusak, R. A.; Lappin, A. G. *J. Phys. Chem.* **1989**, *93*, 6856–6859.

(9) Warren, R. M. L.; Lappin, A. G.; Tatehata, A. *Inorg. Chem.* **1992**, *31*, 1566–1574.

(10) Warren, R. M. L.; Tatehata, A.; Lappin, A. G. *Inorg. Chem.* **1993**, *32*, 1191–1196.

(11) Sysoeva, T. F.; Agre, V. M.; Trunov, V. K.; Dyatlova, N. M.; Fridman, A. Ya. *J. Struct. Chem.* (*Engl. Transl.*) **1986**, *27*, 97–103.

(12) Dwyer, F. P.; Gyarfas, E. C.; Mellor, D. J. *J. Phys. Chem.* **1955**, *59*, 296–297.

(13) Gillard, R. D.; Mithchell, P. R.; Weick, C. F. *J. Chem. Soc., Dalton Trans.* **1974**, 1635–1636.

(14) Jordan, W. T.; Froebe, L. R. *Inorg. Synth.* **1978**, *18*, 96–102.

(15) Work, J. B.; McReynolds, J. P. *Inorg. Synth.* **1946**, *2*, 221–222.

(16) Broomhead, J. A.; Dwyer, F. P.; Hogarth, J. W.; Sievers, R. E. *Inorg. Synth.* **1960**, *6*, 183–188.

(17) Bailar, J. C.; Jones, E. M. *Inorg. Synth.* **1939**, *1*, 37.

(18) Okazaki, H.; Kushi, Y.; Yoneda, H. *J. Am. Chem. Soc.* **1985**, *107*, 4183–4189.

(19) Butler, K. R.; Snow, M. R. *J. Chem. Soc. A* **1971**, 565–569.

(20) Kaufman, G. B.; Takahashi, L. T.; Sugisaka, N. *Inorg. Synth.* **1966**, *8*, 208–209.

(21) Werner, A.; Poupardin, J. *Ber. Dtsch. Chem. Ges.* **1914**, *47*, 1954–1960.

(22) Barton, D.; Harris, G. M. *Inorg. Chem.* **1962**, *1*, 251–255.

(23) Dwyer, F. P.; Sargeson, A. M. *J. Phys. Chem.* **1956**, *60*, 1331–1332.

(24) McCaffery, A. J.; Mason, S. F.; Ballard, R. E. *J. Chem. Soc.* **1965**, 2883–2892.

(25) Smolenaers, P. J.; Beattie, J. K.; Armor, J. N. *Inorg. Synth.* **1979**, *19*, 117–121.

(26) Meyer, T. J.; Taube, H. *Inorg. Chem.* **1968**, *7*, 2369–2379.

0020-1669/94/1333-0227$04.50/0

Table 1. Crystal Data and Intensity Data Collection Parameters

compd	$[\Lambda\text{-Co(en)}_3][\Delta\text{-Co(edta)}]_2\text{Cl}\cdot 10H_2O$
empirical formula	$C_{26}H_{68}ClCo_3N_{10}O_{26}$
fw	1149.14
crystal dimensions, mm	0.13 × 0.19 × 0.51
color	violet
space group	$P2_12_12$ (No. 18)
a, Å	21.046(3)
b, Å	12.813(2)
c, Å	8.158(1)
V, Å^3	2199.9(9)
Z	2
d_{calcd}, g/cm^3	1.74
μ(Mo Kα), cm^{-1}	12.75
no. of total data measd	12791
no. of unique data measd	6037
no. of uniqud data obsd	5263
data/variable ratio	17.6
R_1[a]	0.035
R_2[b]	0.043
goodness of fit	1.17

[a] $R_1 = (\sum|F_o - F_c|/\sum|F_o|)$. [b] $R_2 = (\sum w|F_o - F_c|^2/\sum w|F_o|^2)^{1/2}$.

$[\Lambda\text{-}(+)_{546}\text{-Rh(ox)}_3]\cdot 2H_2O$.[27] The absolute configuration is $[\Delta\text{-}(+)_{350}\text{-Ru(en)}_3]I_3$ ($\epsilon_{310} = 360$ M^{-1} cm^{-1}, $\Delta\epsilon_{328} = +0.87$ M^{-1} cm^{-1}, $\Delta\epsilon_{284} = -2.12$ M^{-1} cm^{-1}).[27] Solutions of $[\Delta\text{-}(+)_{350}\text{-Ru(en)}_3]^{3+}$ were reduced to $[\Delta\text{-}(+)_{375}\text{-Ru(en)}_3]^{2+}$ ($\epsilon_{370} = 120$ M^{-1} cm^{-1}, $\epsilon_{304} = 1020$ M^{-1} cm^{-1}, $\Delta\epsilon_{402} = -0.93$ M^{-1} cm^{-1}, $\Delta\epsilon_{348} = +1.49$ M^{-1} cm^{-1}, $\Delta\epsilon_{284} = +2.32$ M^{-1} cm^{-1})[27] over zinc amalgam. All solutions of $[\text{Ru(en)}_3]^{2+}$ and $[\text{Ru(en)}_3]^{3+}$ were prepared and handled in 0.01 M CF_3SO_3H under an atmosphere of argon gas to prevent air oxidation to the intensely colored $[\text{Ru(en)}_2(C_2N_2H_4)]^{2+}$ ($\epsilon_{448} \approx 7000$ M^{-1} cm^{-1}).[25,28-30] Trifluoromethanesulfonic acid (triflic acid, CF_3SO_3H) was purchased from Alfa, vacuum-distilled,[31] and stored as an approximately 0.75 M aqueous solution.

The kinetics of oxidation of $[\text{Ru(en)}_3]^{2+}$ by $[\text{Co(edta)}]^-$ were investigated under pseudo-first-order conditions using an excess of reductant at 0.10 M ionic strength (CF_3SO_3Na) in the presence of 0.01 M CF_3SO_3H by monitoring the decrease in absorbance of the oxidant at 575 nm with a Durrum Model D-110 stopped-flow spectrophotometer thermostated at 25.0 ± 0.1 °C. Typically, oxidant concentrations were (4–5) × 10^{-5} M, with ruthenium(II) concentrations in the range (4–30) × 10^{-4} M. All solutions were prepared and used under an atmosphere of argon gas, and ruthenium(II) concentrations were determined spectrophotometrically immediately prior to reaction. Plots of $\ln(A - A_\infty)$ against time were generally linear for at least 3 half-lives, and pseudo-first-order rate constants k_{obsd} were calculated from the slopes by least-squares analysis. The reaction stereoselectivity was determined at 25 ± 1 °C with an excess (×3–12) of the racemic oxidant, which was reduced by optically active $[\text{Ru(en)}_3]^{2+}$. Optical activity induced in the unreacted oxidant was determined after the product solution had been passed through a Dowex 50W-X8 strong cation-exchange resin to remove $[\text{Ru(en)}_3]^{3+}$. The reduction of $[\text{Co(edta)}]^-$ by $[\text{Ru(en)}_3]^{2+}$ is faster than the racemization of $[\text{Co(edta)}]^-$, and as a consequence, the more reactive enantiomer of $[\text{Co(edta)}]^-$ is depleted in the reactant pool. This results in a dependence of the observed stereoselectivity on $[\text{Co(edta)}]^-$ concentration, and the correct value of the reaction stereoselectivity is obtained by extrapolation to conditions of infinite excess of the oxidant. Circular dichroism measurements were made on an Aviv 62DS spectrophotometer.

Examination of the crystals of $[\Lambda\text{-Co(en)}_3][\Delta\text{-Co(edta)}]_2\text{Cl}\cdot 10H_2O$ was carried out at 131 ± 2 K on an Enraf-Nonius CAD4 diffractometer equipped with a graphite crystal incident beam monochromator using Mo Kα radiation ($\lambda = 0.710\,73$ Å). A summary of the crystal data and intensity collection parameters is presented in Table 1.[32] The intensity of four representative reflections measured every 60 min showed a small systematic change, and a linear decay correction ranging from 0.971 to 1.000 was applied. Data reduction was done by standard programs.[33] Lorentz and polarization corrections and empirical absorption corrections based on ψ scans were applied to the data. Transmission coefficients from the absorption corrections ranged from 0.941 to 1.000. The positions of the independent cobalt, the cobalt atom on the 2-fold axis at ($^1/_2$, $^1/_2$, z), the chlorine atom at (0, $^1/_2$, z), and 18 of the other 26 non-hydrogen atoms were located from the direct methods solution.[34] The positions for the other non-hydrogen atoms of the two cobalt complexes and the five oxygen atoms of the independent waters of solvation were subsequently located from a series of difference electron density Fourier maps. After preliminary refinement, positions for nearly all the hydrogen atoms could be found in a difference electron density Fourier map. The structure was refined by a full-matrix least-squares process. Final cycles of least-squares refinement assigned anisotropic displacement parameters to all non-hydrogen atoms and included hydrogen atom coordinates and isotropic displacement parameters as fixed parameters. The highest peak in the final difference electron density Fourier map was 0.87 e/Å^3. Refinement of the other enantiomorph converged with $R_1 = 0.050$ and $R_2 = 0.062$, confirming the veracity of the enantiomorph reported.

Results

Oxidation of $[\text{Ru(en)}_3]^{2+}$ by an excess of $[\text{Co(edta)}]^-$ and subsequent recovery of unreacted $[\text{Co(edta)}]^-$ yield a stoichiometry of 0.94 ± 0.09 based on initial concentration of $[\text{Ru(en)}_3]^{2+}$. This is consistent with the expected 1:1 single-electron-transfer process

$$[\text{Ru(en)}_3]^{2+} + [\text{Co(edta)}]^- \xrightarrow{k_{12}} [\text{Ru(en)}_3]^{3+} + [\text{Co(edta)}]^{2-} \tag{1}$$

Pseudo-first-order rate constants, k_{obsd}, for the oxidation of $[\text{Ru(en)}_3]^{2+}$ by $[\text{Co(edta)}]^-$ at 25.0 °C and 0.10 M ionic strength are available as supplementary material. A plot of k_{obsd} against $[[\text{Ru(en)}_3]^{2+}]$ is linear with a negligible intercept, and the second-order rate constant, k_{12}, is (6.0 ± 0.1) × 10^3 M^{-1} s^{-1}. Addition of NaI does not affect the rate of the reaction. Some experiments were also carried out on the oxidation of $[\text{Ru(en)}_3]^{2+}$ by $[\text{Co(ox)}_3]^{3-}$, where the reaction is rapid, close to the limit of the stopped-flow technique. At low ruthenium(II) concentrations, 5.0 × 10^{-4} M, the half-life of the reaction is ≈2 ms, which corresponds to a second-order rate constant of ≈7 × 10^5 M^{-1} s^{-1}. This contrasts with an earlier study in which the rate of this reaction is reported as 0.055 M^{-1} s^{-1} at 25 °C and 0.20 M ionic strength.[35] It should be noted that, in this earlier study, the rate was determined with an excess of oxidant and monitored at the absorption maximum of the reductant (302 nm). $[\text{Co(ox)}_3]^{3-}$ absorbs strongly at this wavelength ($\epsilon_{302} \approx 2 \times 10^3$ M^{-1} cm^{-1}) and undergoes photodecomposition upon irradiation with 302-nm light in the absence of $[\text{Ru(en)}_3]^{2+}$ on a time scale consistent with the quoted rate.

There have been several reports of stereoselective oxidation of $[\text{Co(en)}_3]^{2+}$ by optically active oxidants.[3,4,10,36,37] Typically these are carried out with a large excess of the substitution-labile $[\text{Co(en)}_3]^{2+}$ and determined by isolation of the inert product, $[\text{Co(en)}_3]^{3+}$. For the substitution-inert reductant $[\text{Ru(en)}_3]^{2+}$, a comparable experiment entails anaerobic separation of $[\text{Ru(en)}_3]^{3+}$ from $[\text{Ru(en)}_3]^{2+}$, and the high self-exchange rate[38] of

---

(27) Elsbernd, H.; Beattie, J. K. *Inorg. Chem.* **1969**, *8*, 893–899.

(28) Pladziewicz, J. R.; Meyer, T. J.; Broomhead, J. A.; Taube, H. *Inorg. Chem.* **1973**, *12*, 639–643.

(29) Elsbernd, H.; Beattie, J. K. *J. Chem. Soc. A* **1970**, *2598*–2600.

(30) Lane, B. C.; Lester, J. E.; Basolo, F. *J. Chem. Soc., Chem. Commun.* **1971**, 1618–1619.

(31) Dixon, N. E.; Lawrance, G. A.; Lay, P. A.; Sargeson, A. M.; Taube, H. *Inorg. Synth.* **1986**, *24*, 243–250.

(32) Data were collected by the θ–2θ scan technique to a maximum 2θ value of 58.7°. Data with $F_o > 3\sigma(F_o)$ were considered observed. Hydrogen atoms were included in the final refinement cycles as idealized contributions with d(C–H) = 0.98 Å, d(N–H) = 0.87 Å, and B(H) = 1.1B(attached atom). All calculations were performed on a VAXstation 3200 using the SDP/VAX program system.

(33) Frenz, B. A. The Enraf-Nonius CAD4 SDP—A Real-Time System for Concurrent X-Ray Data Collection and Crystal Structure Determination. In *Computing in Crystallography*; Schenk, H., Olthof-Hazelkamp, R., van Konigsveld, H., Bassi, G. C., Eds.; Delft University Press: Delft, Holland, 1978; pp 64–71.

(34) Sheldrick, G. *SHELXS-86*; Institut für Anorganische Chemie der Universität: Gottingen, Germany, 1986.

(35) Ehighaokhuo, J. O.; Ojo, J. F.; Olubyide, O. *J. Chem. Soc., Dalton Trans.* **1985**, 1665–1667.

(36) Marusak, R. A.; Osvath, P.; Kemper, M.; Lappin, A. G. *Inorg. Chem.* **1989**, *28*, 1542–1548.

(37) Tatehata, A.; Mitani, T. *Chem. Lett.* (*Jpn*) **1989**, 1167–1170.

(38) Beattie, J. K.; Smolenaers, P. J. *J. Phys. Chem.* **1986**, *90*, 3684–3686.

Table 2. Stereoselectivity in the Oxidation of $[\Delta\text{-}(+)_{375}\text{-Ru(en)}_3]^{2+}$ by $[\text{Co(edta)}]^-$ [a]

$10^4[[\Delta\text{-}(+)_{375}\text{-Ru(en)}_3]^{2+}]$, M	$10^4[[\text{Co(edta)}]^-]$, M	$10^4[\text{I}^-]$, M	S[b]	stoichiom
16.6	62.8	50	1.3% ΔΛ	0.91
11.9	74.8	36	1.9% ΔΛ	0.72
11.9	73.0	321	1.6% ΔΛ	0.98
11.9	71.1	607	2.3% ΔΛ	0.98
6.9	87.3	21	2.1% ΔΛ	1.10
			2.2(3)% ΔΛ[c]	0.94(9)

[a] 25 ± 1 °C, 0.10 M ionic strength (CF_3SO_3Na), 0.01 M CF_3SO_3H. [b] Stereoselectivity expressed as enantiomeric excess for the favored reaction. [c] Extrapolation to infinite excess of oxidant.

Table 3. Fractional Orthorhombic Coordinates and Isotropic Atomic Displacement Parameters (Å^2) for the Non-Hydrogen Atoms[a]

atom	x	y	z	B_{iso}
Co1	$^1/_2$	$^1/_2$	0.65816(6)	0.828(7)
N1	0.5663(1)	0.5193(2)	0.8237(3)	1.12(4)
C1	0.5793(1)	0.4192(2)	0.9069(3)	1.34(5)
C2	0.5798(1)	0.3371(2)	0.7722(4)	1.31(5)
N2	0.5219(1)	0.3516(2)	0.6700(3)	1.12(4)
N3	0.5619(1)	0.5214(2)	0.4820(3)	1.06(4)
C3	0.5334(2)	0.4936(4)	0.3231(5)	4.29(9)
Co2	0.75989(2)	0.90112(2)	0.66717(4)	0.760(5)
O1	0.81510(9)	0.9796(2)	0.7979(2)	1.16(3)
C8	0.8070(1)	1.0792(2)	0.7953(3)	1.22(5)
O2	0.8413(1)	1.1415(2)	0.8666(3)	1.93(4)
C7	0.7506(1)	1.1167(2)	0.6963(3)	1.04(4)
N7	0.7134(1)	1.0279(2)	0.6268(3)	0.87(4)
C9	0.7099(1)	1.0360(2)	0.4450(3)	1.07(4)
C10	0.7747(1)	1.0011(2)	0.3798(3)	1.05(4)
O3	0.80661(8)	0.9400(1)	0.4750(2)	1.04(3)
O4	0.79356(9)	1.0308(2)	0.2454(3)	1.48(4)
C11	0.6523(1)	1.0143(2)	0.7159(3)	1.09(4)
C12	0.6683(1)	0.9657(2)	0.8809(3)	1.00(4)
N8	0.7045(1)	0.8678(2)	0.8456(3)	0.95(4)
C13	0.7468(1)	0.8294(2)	0.9786(3)	1.06(4)
C14	0.7982(1)	0.7644(2)	0.8954(4)	1.12(4)
O5	0.80601(9)	0.7806(2)	0.7400(2)	1.20(3)
O6	0.83008(9)	0.7030(2)	0.9769(3)	1.43(4)
C15	0.6612(1)	0.7814(2)	0.7922(3)	1.20(5)
C16	0.6611(1)	0.7719(2)	0.6080(4)	1.15(5)
O7	0.70549(9)	0.8212(1)	0.5338(2)	1.10(3)
O8	0.6207(1)	0.7180(2)	0.5394(3)	1.85(4)
Cl	0	$^1/_2$	0.6167(2)	2.88(2)
O1s	0.5378(1)	0.7094(2)	1.0260(3)	3.26(5)
O2s	0.9502(1)	0.6179(2)	0.9519(3)	2.64(5)
O3s	0.4207(1)	0.7715(2)	1.4210(4)	3.89(6)
O4s	0.6117(1)	0.8578(2)	0.2287(3)	2.50(5)
O5s	0.5181(2)	0.8760(3)	−0.2625(4)	4.82(8)

[a] Estimated standard deviations in the least significant digits are given in parentheses. Thermal parameters for the anisotropically refined atoms are given in the form of the isotropic equivalent displacement parameter defined as $^4/_3[a^2B_{11} + b^2B_{22} + c^2B_{33} + ab(\cos\gamma)B_{12} + ac(\cos\beta)B_{13} + bc(\cos\alpha)B_{23}]$.

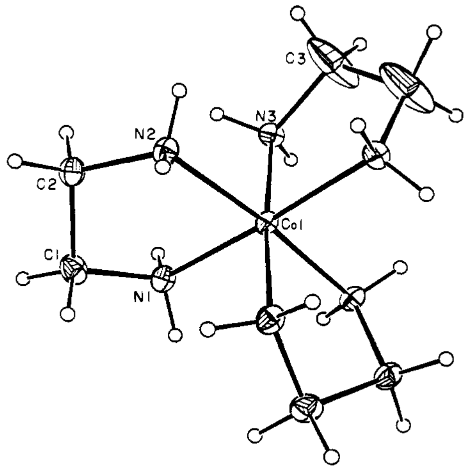

Figure 1. Ortep drawing of the $[\Lambda\text{-Co(en)}_3]^{3+}$ cation showing the numbering scheme. Thermal ellipsoids are drawn to illustrate 50% probability surfaces. Hydrogen atoms are drawn arbitrarily small for clarity.

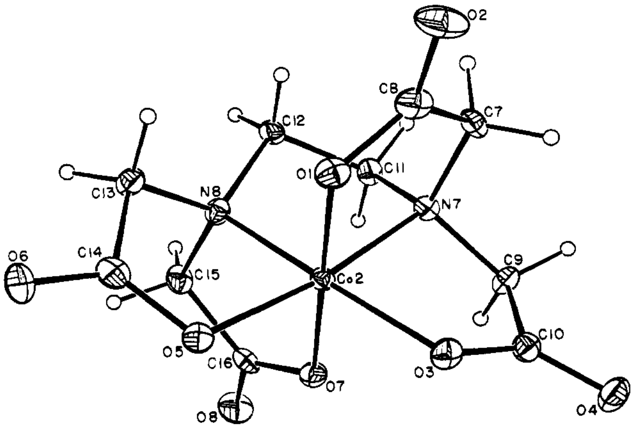

Figure 2. Ortep drawing of the $[\Delta\text{-Co(edta)}]^-$ anion showing the numbering scheme. Thermal ellipsoids are drawn to illustrate 50% probability surfaces. Hydrogen atoms are drawn arbitrarily small for clarity.

$[\text{Ru(en)}_3]^{3+/2+}$ would result in rapid loss of any optical activity induced in the $[\text{Ru(en)}_3]^{3+}$ produced. Consequently, the stereoselectivity was determined by measuring optical activity induced by $[\Delta\text{-}(+)_{375}\text{-Ru(en)}_3]^{2+}$ in an excess of $[\text{Co(edta)}]^-$, and values obtained under a variety of different conditions are summarized in Table 2. Extrapolation to conditions of infinite excess of the oxidant yields a 2.2 ± 0.3% stereoselectivity with a ΔΛ preference. Within the error of the experiment, there is no effect of adding iodide ion. Similar experiments with $[\text{Co(ox)}_3]^{3-}$ were attempted; however, the combination of the more rapid rate of racemization of $[\text{Co(ox)}_3]^{3-}$ and the high-dilution conditions required to avoid precipitation with $[\text{Ru(en)}_3]^{3+}$ precluded any determination of stereoselectivity in this reaction.

Early reports of resolution of $[\text{Co(edta)}]^-$ involved the use of $[\text{Co(en)}_3]^{3+}$ as resolving agent and isolation of a salt of composition $[\Lambda\text{-}(+)_{589}\text{-Co(en)}_3][\Delta\text{-}(+)_{546}\text{-Co(edta)}]_2\text{Cl}\cdot4\text{H}_2\text{O}$.[12] Preparation of the more soluble $[\Lambda\text{-}(+)_{589}\text{-Co(en)}_3][\Lambda\text{-}(-)_{546}\text{-Co(edta)}]_2\text{Cl}\cdot n\text{H}_2\text{O}$ has also been reported,[39] but crystals of this diastereomeric pair have not been obtained. The salt characterized crystallographically in this study has composition $[\Lambda\text{-}(+)_{589}\text{-Co(en)}_3][\Delta\text{-}(+)_{546}\text{-Co(edta)}]_2\text{Cl}\cdot10\text{H}_2\text{O}$. It readily effloresces by loss of water, and it is likely that the compounds isolated by Dwyer and Bailar and their co-workers correspond to partially dehydrated samples.

Fractional crystallographic coordinates and isotropic atomic displacement parameters for $[\Lambda\text{-Co(en)}_3][\Delta\text{-Co(edta)}]_2\text{Cl}\cdot10\text{H}_2\text{O}$ are collected in Table 3. The $[\text{Co(en)}_3]^{3+}$ cation[40–43] and $[\text{Co(edta)}]^-$ anion[44,45] have bond lengths and angles within normal limits (Table 4), and the numbering schemes for the ions are shown in Figures 1 and 2. The absolute configuration of the cation is Λ with two of the 1,2-diaminoethane rings in the λ (*ob*) conformation. The third ring shows evidence for disorder between λ and δ (*ob* and *lel*, respectively), and the apparent shortness of

---

(39) Kirschner, S.; Wei, Y.-K.; Bailar, J. C. *J. Am. Chem. Soc.* **1957**, *79*, 5877–5880.

(40) Iwata, M.; Nakatsu, K.; Saito, Y. *Acta Crystallogr.* **1969**, *B25*, 2562–2571.

(41) Whuler, P. A.; Spinat, P.; Brouty, C. *Acta Crystallogr.* **1980**, *B36*, 1086–1091.

(42) Mizuta, T.; Tada, T.; Kushi, Y.; Yoneda, H. *Inorg. Chem.* **1988**, *27*, 3836–3841.

(43) Lappin, A. G.; Haller, K. J.; Warren, R. M. L.; Tatehata, A. *Inorg. Chem.* **1993**, *32*, 4498–4504.

(44) Weakliem, H. A.; Hoard, J. L. *J. Am. Chem. Soc.* **1959**, *81*, 549–555.

(45) Okamoto, K.; Tsukihara, T.; Hidaka, J.; Shimura, Y. *Chem. Lett.* (*Jpn.*) **1973**, 145–148.

Table 4. Selected Interatomic Distances (Å) and Interatomic Angles (deg)[a]

	Distances		
Co1–N1	1.958(2)	C7–N7	1.492(3)
Co1–N2	1.958(2)	N7–C9	1.488(3)
Co1–N3	1.959(2)	N7–C11	1.488(3)
N1–C1	1.477(3)	C9–C10	1.530(3)
C1–C2	1.521(4)	C10–O3	1.291(3)
C2–N2	1.489(3)	C10–O4	1.226(3)
N3–C3	1.473(4)	C11–C12	1.520(4)
C3–C3′	1.414(7)	C12–N8	1.494(3)
Co2–O1	1.871(2)	N8–C13	1.489(3)
Co2–N7	1.925(2)	N8–C15	1.498(3)
Co2–O3	1.916(2)	C13–C14	1.525(4)
Co2–N8	1.913(2)	C14–O5	1.295(3)
Co2–O5	1.919(2)	C14–O6	1.229(3)
Co2–O7	1.882(2)	C15–C16	1.508(4)
O1–C8	1.287(3)	C16–O7	1.280(3)
C8–O2	1.224(3)	C16–O8	1.230(3)
C8–C7	1.514(4)		
	Angles		
N1–Co1–N2	85.45(9)	Co2–N7–C7	108.2(1)
N1–Co1–N3	90.79(8)	Co2–N7–C9	104.7(2)
N2–Co1–N3	90.9(1)	Co2–N7–C11	104.8(2)
Co1–N1–C1	109.9(2)	C7–N7–C9	110.6(2)
N1–C1–C2	105.7(2)	C7–N7–C11	110.9(2)
C1–C2–N2	108.2(2)	C9–N7–C11	116.9(2)
Co1–N2–C2	110.0(2)	N7–C9–C10	106.4(2)
Co1–N3–C3	109.9(2)	C9–C10–O3	115.5(2)
N3–C3–C3′	112.2(3)	C9–C10–O4	120.6(2)
O1–Co2–N7	87.65(9)	O3–C10–O4	123.9(2)
O1–Co2–O3	90.44(8)	Co2–O3–C10	112.5(2)
O1–Co2–N8	93.72(9)	N7–C11–C12	106.8(2)
O1–Co2–O5	86.68(8)	C11–C12–N8	106.6(2)
O1–Co2–O7	179.05(8)	Co2–N8–C12	105.7(2)
N7–Co2–O3	84.32(8)	Co2–N8–C13	105.3(1)
N7–Co2–N8	90.49(9)	Co2–N8–C15	108.3(2)
N7–Co2–O5	171.74(9)	C12–N8–C13	116.2(2)
N7–Co2–O7	92.96(8)	C12–N8–C15	111.5(2)
O3–Co2–N8	173.22(9)	C13–N8–C15	109.3(2)
O3–Co2–O5	101.71(8)	N8–C13–C14	106.3(2)
O3–Co2–O7	88.91(8)	C13–C14–O5	116.0(2)
N8–Co2–O5	83.89(8)	C13–C14–O6	119.7(2)
N8–Co2–O7	86.99(9)	O5–C14–O6	124.3(3)
O5–Co2–O7	92.78(8)	Co2–O5–C14	111.6(2)
Co2–O1–C8	116.2(2)	N8–C15–C16	110.5(2)
O1–C8–O2	124.0(3)	C15–C16–O7	115.4(2)
O1–C8–C7	115.3(2)	C15–C16–O8	120.0(3)
O2–C8–C7	120.6(2)	O7–C16–O8	124.5(3)
C8–C7–N7	111.8(2)	Co2–O7–C16	116.1(2)

[a] Estimated standard deviations in the least significant digits are given in parentheses.

the C3–C3′ bond is a consequence of the averaging of the two conformations. The absolute configuration for the anion is ΔΛΔ, abbreviated to Δ. The 1,2-diaminoethane backbone has the λ conformation, while the in-plane G rings and the out-of-plane R rings are best described as having envelope conformations.

The packing in [Λ-(+)$_{589}$-Co(en)$_3$][Δ-(+)$_{546}$-Co(edta)]$_2$Cl·10H$_2$O consists of alternating sheets of complex cations and anions, which stack along the crystallographic *a* axis. The C_2 axis of the [Co(en)$_3$]$^{3+}$ cation is aligned parallel to the crystallographic *c* axis, as required by the crystallographically imposed symmetry. Solvent molecules and the chloride ion alternate with the cation along the *b* axis. A network of hydrogen bonds between cations and anions extends throughout the *ab* plane, and hydrogen bonding to solvent water connects these sheets along the *c* axis. Two different cation–anion hydrogen-bonding interactions are observed. At a Co–Co distance of 5.85 Å the [Co(en)$_3$]$^{3+}$ ion sustains hydrogen-bonding contacts from a C_3 axis N–H and a C_2 axis N–H with the terminal and metal-bound oxygens on one of the G carboxylate arms of [Co(edta)]$^-$. However, it is the C_2 axis of [Co(en)$_3$]$^{3+}$ which approaches [Co(edta)]$^-$ most directly. This closest interaction is depicted in Figure 3a. At 7.51 Å a terminal oxygen atom from an R carboxylate arm of [Co(edta)]$^-$ interacts with protons on the pseudo-C_3 face of [Co(en)$_3$]$^{3+}$. No hydrogen bonding is observed between [Co(edta)]$^-$ complex ions. Possible hydrogen-bonding contacts in [Λ-(+)$_{589}$-Co(en)$_3$][Δ-(+)$_{546}$-Co(edta)]$_2$Cl·10H$_2$O are listed in Table 5.

Table 5. Possible Hydrogen-Bonding Interactions in [Λ-(+)$_{589}$-Co(en)$_3$[Δ-(+)$_{546}$-Co(edta)]$_2$Cl·10H$_2$O[a]

A···H–B	A–B, Å	A–H, Å	A–H–B, deg	Co–Co, Å
O4···H1c–N1	3.01	2.21	147.6	5.85
O3···H3d–N3	2.98	2.13	158.4	5.85
O8···H2c–N2	3.31	2.77	120.1	7.51
O8···H3c–N3	2.85	1.99	159.5	7.51
O1s···H2c–N2	3.26	2.62	129.1	
O3s···H2d–N2	2.84	2.04	148.1	
O5s···H2c–N2	3.09	2.47	126.3	
O2···H–O1s	2.83			
O2···H–O4s	3.04			
O5···H–O3s	2.83			

[a] The definition of what constitutes hydrogen bonding is broad, and criteria for assigning hydrogen bonding interactions in crystals such as these have been outlined previously.[43]

Discussion

The rate of oxidation of [Ru(en)$_3$]$^{2+}$ by [Co(edta)]$^-$ is first order in both reagents with a second-order rate constant of 6.0 × 10^3 M^{-1} s^{-1} at 25.0 °C and 0.10 M ionic strength. Electron transfer takes place much faster than the rate of substitution on either complex and indicates that the reaction is outer-sphere in nature. Values for reduction potentials and self-exchange rate constants for [Co(edta)]$^{-/2-}$ and [Ru(en)$_3$]$^{3+/2+}$ are available[38,46–48] and allow a comparison of the rate with the predictions of the Marcus expression[49]

$$k_{12} = (k_{11}k_{22}K_{12}f_{12})^{1/2} \tag{2}$$

where k_{12} is the cross-reaction rate, K_{12} is the equilibrium constant for the reaction, k_{11} and k_{22} are the self-exchange rates, and $\ln(f_{12}) = \{\ln(K_{12})\}^2/\{4\ln(k_{11}k_{22}/Z^2)\}$ where Z is the collision frequency for neutral molecules in solution, $\approx 10^{11}$ M^{-1} s^{-1}. A second-order rate constant of 50 M^{-1} s^{-1} is calculated for the reaction at 25 °C and 0.10 M ionic strength after allowance for appropriate electrostatic work terms.[50] This is 2 orders of magnitude lower than the observed rate constant and lies outside the range of variation normally expected. One potential source of uncertainty is the poorly defined self-exchange rate for [Co(edta)]$^{-/2-}$.[38,51] However, reference to Table 6, where data for a number of reactions of [Co(edta)]$^-$ are collected, reveals that good agreement between observed and calculated rates is found with reductants which are anionic or are not capable of hydrogen-bond formation. Calculated rates for reductants which are capable of formation of hydrogen bonds[3,4,10,55] with [Co(edta)]$^-$

---

(46) Weaver, M. J.; Nettles, S. M. *Inorg. Chem.* **1980**, *19*, 1641–1646.
(47) Im, Y. A.; Busch, D. H. *J. Am. Chem. Soc.* **1961**, *83*, 3357–3362.
(48) Ogino, H.; Ogino, K. *Inorg. Chem.* **1983**, *22*, 2208–2211.
(49) Sutin, N. *Acc. Chem. Res.* **1982**, *15*, 275–282.
(50) Brown, G. M.; Sutin, N. *J. Am. Chem. Soc.* **1979**, *101*, 883–892.
(51) Jolley, W. H.; Stranks, D. R.; Swaddle, T. W. *Inorg. Chem.* **1992**, *31*, 507–511.
(52) Lannon, A. M.; Lappin, A. G.; Segal, M. G. *Inorg. Chem.* **1984**, *23*, 4167–4170.
(53) Huchital, D. H.; Lepore, J. *Inorg. Chem.* **1978**, *17*, 1134–1138.
(54) Dimmock, P. W.; McGinnis, J.; Ooi, B.-L.; Sykes, A. G. *Inorg. Chem.* **1990**, *29*, 1085–1089.
(55) Armstrong, G. D.; Sinclair-Day, J. D; Sykes, A. G. *J. Phys. Chem.* **1986**, *90*, 3805–3808.
(56) Warren, R. M. L.; Opiteck, G. J.; Öhrström, L.; Tatehata, A.; Lappin, A. G. To be published.
(57) Toma, H. E.; Lellis, F. T. P. *Polyhedron*, **1985**, *4*, 993–997.
(58) Campion, R. J.; Deck, C. F.; King, P.; Wahl, A. C. *Inorg. Chem.* **1967**, *6*, 672–681.
(59) Takagi, H.; Swaddle, T. W. *Inorg. Chem.* **1992**, *31*, 4669–4673.

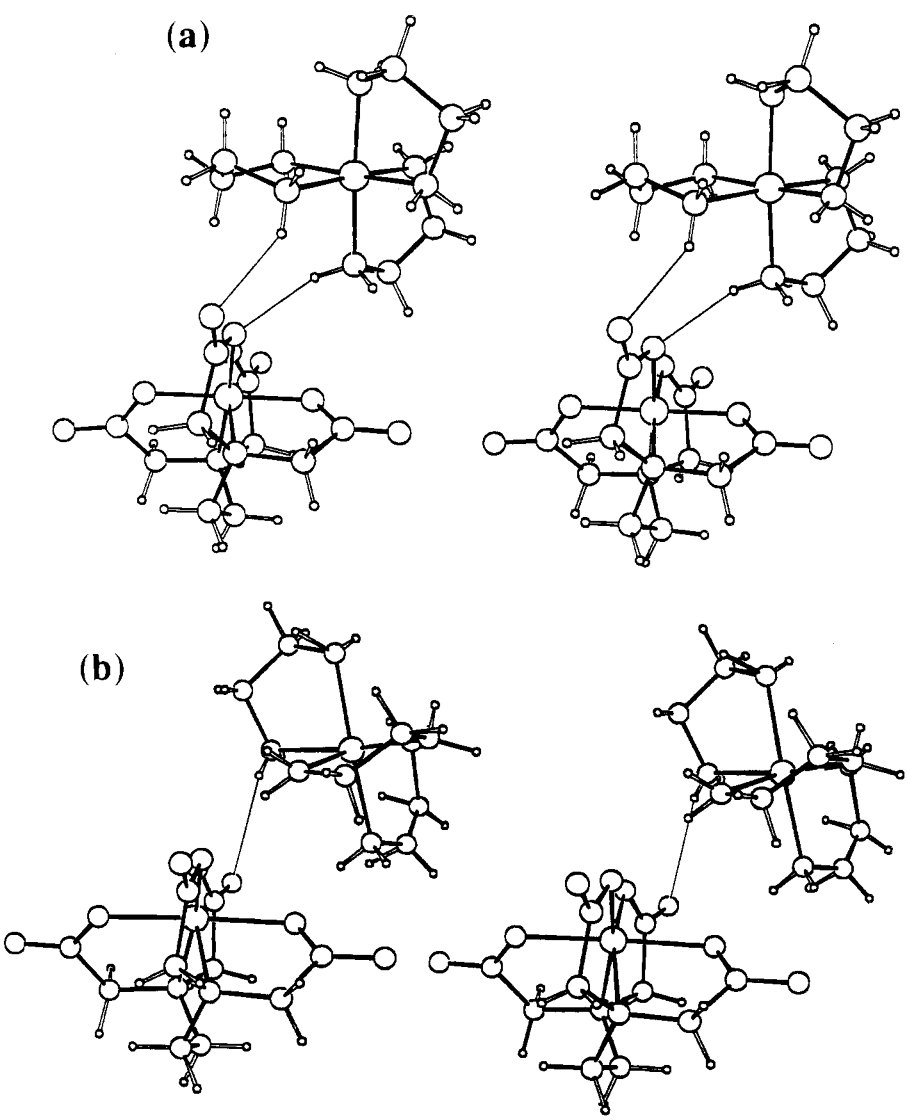

Figure 3. Stereoviews showing the closest anion–cation hydrogen-bonding interactions in (a) [Λ-Co(en)$_3$][Δ-Co(edta)]$_2$Cl·10H$_2$O and (b) [Δ-Ni(en)$_3$][Δ-Ni(edta)]·4H$_2$O. The views are at right angles to the C_2 axes of the [Co(edta)]$^-$ and [Ni(edta)]$^-$ complexes, which are shown on the bottom of each pair. The strongest hydrogen bonds are shown by single lines.

range from 10 to 10^2 times lower than the observed rates. It seems likely that additional hydrogen-bonding stabilization in the electron-transfer precursor results in rate enhancement. Effects of this magnitude can be expected as a result of hydrogen bonding.[10]

Stereoselectivity measured in the oxidation of [Δ-(+)$_{375}$-Ru(en)$_3$]$^{2+}$ by [Co(edta)]$^-$ is a modest 2% $\Delta\Lambda$, corresponding to $k_{\Delta\Lambda}/k_{\Delta\Delta} = 1.04$. Although, in the same sense, it is significantly smaller than in the analogous reaction with [Co(en)$_3$]$^{2+}$, where estimates of the stereoselectivity from three independent studies range between 9% $\Delta\Lambda$ and 11% $\Delta\Lambda$ with $k_{\Delta\Lambda}/k_{\Delta\Delta} \approx 1.22$.[3,4,37] If these reaction stereoselectivities are determined exclusively by chiral recognition in the electron-transfer precursor, they must reflect the trends observed for stereoselectivity in ion-pairing measurements; otherwise, a more complex picture will emerge. Measurements of the chiral recognition in ion-pair formation between [Co(edta)]$^-$ and [Co(en)$_3$]$^{3+}$ have been reported[7] and range from $K_{\Delta\Lambda}/K_{\Delta\Delta} = 1.06 \pm 0.03$ at 0.01 M ionic strength to $K_{\Delta\Lambda}/K_{\Delta\Delta} = 1.18 \pm 0.08$ at 0.05 M ionic strength. Extrapolation to 0.1 M ionic strength projects an enantiomeric excess of 12%

Table 6. Parameters Used in Marcus Calculations (25 °C)[a]

reductant (1)	oxidant (2)	k_{12}(obsd)[b] $M^{-1}\,s^{-1}$	k_{12}(calcd), $M^{-1}\,s^{-1}$	k_{12}(obsd)/k_{12}(calcd)	ref
[V(pic)$_3$]$^-$	[Co(edta)]$^-$	6.5×10^4	2×10^5	0.3	52
[Fe(CN)$_6$]$^{4-}$	[Co(edta)]$^-$	0.173	7×10^{-2}	2	53
[Fe(edta)]$^{2-}$	[Co(edta)]$^-$	3.7	3	1	54
[Ru(en)$_3$]$^{2+}$	[Co(edta)]$^-$	6.0×10^3	50	120	this work
[Co(en)$_3$]$^{2+}$	[Co(edta)]$^-$	18	2	9	10
[Co(sep)]$^{2+}$	[Co(edta)]$^-$	8.26×10^4	1×10^3	80	55
[Co(tacn)$_2$]$^{2+}$	[Co(edta)]$^-$	2.76×10^4	3×10^3	9	55
[Co(phen)$_3$]$^{2+}$	[Co(edta)]$^-$	3×10^{-3}	1×10^{-2}	0.3	56

[a] Reduction potentials (V), self-exchange rates ($M^{-1}\,s^{-1}$), and radii (Å) used in electrostatics-corrected Marcus calculations: [V(pic)$_3$]$^{0/-}$, –0.41, 9.7×10^5, 6;[52,57] [Fe(CN)$_6$]$^{4-}$, 0.42, 1.9×10^4, 4.1;[58,59] [Fe(edta)]$^{2-}$, 0.12, 4.5×10^3, 5;[54,60] [Ru(en)$_3$]$^{2+}$, 0.17, 1.7×10^4, 3.8;[38,46] [Co(en)$_3$]$^{2+}$, –0.18, 7.7×10^{-5}, 3.8,[61–63] [Co(sep)]$^{2+}$, –0.30, 5.1, 5;[64] [Co(tacn)$_2$]$^{2+}$, –0.41, 0. 19, 4;[65] [Co(phen)$_3$]$^{2+}$, 0.36, 12.0, 7.2;[66] [Co(edta)]$^-$, 0.37, 2×10^{-7}, 5.[47,48] pic$^-$ = 2-, picolinate (1–), tacn = 1,4,7-triazacyclononane, phen = 1,10-phenanthroline. [b] Corrected to 0.10 M ionic strength.

---

(60) Schwarzenbach, G.; Heller, J. *Helv. Chim. Acta* **1951**, *34*, 576–591.
(61) Creaser, I. I.; Sargeson, A. M.; Zanella, A. W. *Inorg. Chem.* **1983**, *22*, 4022–4029.
(62) Dwyer, F. P.; Sargeson, A. M. *J. Phys. Chem.* **1961**, *65*, 1892–1894.
(63) Jolley, W. H.; Stranks, D. R.; Swaddle, T. W. *Inorg. Chem.* **1990**, *29*, 385–389.
(64) Creaser, I. I.; Harrowfield, J. M.; Herlt, A. J.; Sargeson, A. M.; Springborg, J.; Geue, R. J.; Snow, M. R. *J. Am. Chem. Soc.* **1982**, *104*, 6016–6025.
(65) Küppers, H.-J.; Neves, A.; Pomp, C.; Ventur, D.; Wieghardt, K.; Nuber, B.; Weiss, J. *Inorg. Chem.* **1986**, *25*, 2400–2408.
(66) Warren, R. M. L.; Lappin, A. G.; Dev Mehta, B.; Neumann, H. M. *Inorg. Chem.* **1990**, *29*, 4185–4189.

ΔΛ for the ion pair, showing closer agreement with the stereoselectivity for reduction by $[Co(en)_3]^{2+}$ than by $[Ru(en)_3]^{2+}$. However, stereoselectivity has been shown to be very sensitive to the conformation of the chelate rings.[3,36] In the reductions of $[Co(edta)]^-$ by $[Co(chxn)_3]^{2+}$ and $[Co(bn)]^{2+}$ (bn = *trans*-2,3-diaminobutane), for which isomers with different chelate ring conformations can be isolated, stereoselectivity changes from a homochiral or ΔΔ preference to a heterochiral or ΔΛ preference as the *ob* character of the ligand conformations changes from lel_3 to ob_3. Both $[Co(en)_3]^{2+}$ and $[Ru(en)_3]^{2+}$ are believed to exist predominantly in the lel_2ob form in solution,[67] but the larger ion is expected to have more *ob* character. Structural studies of $[Ru(en)_3]^{2+}$ and $[Co(en)_3]^{2+}$ reveal that the Co–N bond length in the latter complex[68] averages 0.03 Å greater than Ru–N.[69] Consequently, on the basis of ring conformation, reduction by $[Co(en)_3]^{2+}$ should result in a larger ΔΛ stereoselectivity, in good agreement with the experimental observations. Although contributions from other factors cannot be excluded and indeed are expected,[70] in this instance the differences in chiral induction are readily explained by differences in chiral recognition in the electron-transfer precursor.

The electron-transfer precursor has no single well-defined structure; rather, it is envisaged as a weighted assembly of many structures, each with its own thermodynamic stability and electron-transfer reactivity. It may seem inappropriate to look to the results of crystal structure analysis for an explanation for differences in solution reactivity, and clearly caution must be exercised. However, in this instance, reference to the crystal structure provides some important clues to the types of interactions which might be expected to occur in solution, and formation of the crystals is also the result of a stereoselective process in which ion-pair formation is the initial step.

Individual component ions of $[\Lambda\text{-}(+)_{589}\text{-}Co(en)_3][\Delta\text{-}(+)_{546}\text{-}Co(edta)]_2Cl\cdot 10H_2O$ have normal bond lengths and angles, and further comment is not required. The principal interest in this structure lies in the interactions between the complex ions and evidence from hydrogen-bonding or other interactions which might cast light on the mechanism of chiral discrimination. The X-ray structure reveals that there are two close contact interactions. The closest of these, illustrated in Figure 3a, is of particular relevance. Relative to $[Co(edta)]^-$, the $[Co(en)_3]^{3+}$ ion lies off-center on one of the pseudo-C_3 carboxylate faces. In the determination of the solution ion-pair structure by the effect of paramagnetic $[Cr(en)_3]^{3+}$ on the ^1H NMR spectrum of $[Co(edta)]^-$, a similar orientation of the paramagnetic center toward $[Co(edta)]^-$ was found to be preferred.[8] Thus there is a direct link between the crystal and solution orientations.

An interesting comparison can also be drawn with the crystal structure of the related salt $[\Delta\text{-}Ni(en)_3][\Delta\text{-}Ni(edta)]\cdot 4H_2O$, which has been published previously.[11] The conformation of the 1,2-diaminoethane rings in $[Ni(en)_3]^{2+}$ is Δ(δλλ), or lel_2ob. As with the cobalt salt, two different cation–anion hydrogen-bonding interactions are observed. At a nickel–nickel distance of 5.40 Å a pseudo-C_3 face of the $[Ni(en)_3]^{2+}$ cation lies slightly offset from a pseudo-C_3 carboxylate face of the $[Ni(edta)]^{2-}$ anion and forms hydrogen bonds with oxygen atoms on a G and an R carboxylate arm forming this face. At 6.14 Å the other pseudo-C_3 face of the $[Ni(en)_3]^{2+}$ cation interacts with the terminal and metal-bound oxygen atoms of an R carboxylate arm of $[Ni(edta)]^{2-}$. The closer and most relevant of the two interactions is shown in Figure 3b, and the similarities with Figure 3a and the solution orientation are a recurring feature.

These two structures provide one example of a heterochiral interaction (ΔΛ) and one example of a homochiral interaction (ΔΔ). Although there are significant differences in charge, stoichiometry, and counterions, a comparison between the two is instructive. For the ΔΛ pair the closest interaction involves one of the C_2 axes of the cation, whereas for the ΔΔ pair the closest interaction is with one of the C_3 faces. There are two points to make. The first is that although the absolute configurations of the cations differ, in the closest interaction with the anion, the helicity presented by the chelate rings is $P(C_2)$ for $[Co(en)_3]^{3+}$ and $P(C_3)$ for $[Ni(en)_3]^{2+}$ where P describes clockwise helicity as opposed to *M* or anticlockwise helicity. In other words, helicity is conserved in the interaction with the pseudo-C_3 carboxylate face of the anion despite the change in orientation. A similar observation was made in a structural analysis of the diastereomeric interactions of $[Co(en)_3]^{3+}$ with $[Co(ox)_2(en)]^-$.[38] The second point is that the chelate ring conformations in the cations are dependent on whether the dominant interaction involves the C_3 face (lel_2ob) or the C_2 face ($lelob_2/ob_3$). Strong hydrogen-bond formation along the C_3 axis is known to promote *lel* character.[71–73] These two observations combine to provide a rationalization for the strong chelate ring conformation dependence of stereoselectivity in reactions fo the species.[3] The success of this rationalization lends further credence for the use of the X-ray data in interpreting the chiral discrimination.

In conclusion, stereoselectivities in the reductions of $[Co(edta)]^-$ by $[Co(en)_3]^{2+}$ and $[Ru(en)_3]^{2+}$ are modest and are dominated by chiral recognition in the electron-transfer precursor assembly. There is evidence for strong hydrogen-bonding interactions between the reactions in this assembly. The proposed mechanism for chiral recognition arises from differences in the preferred orientation of the cation with the carboxylate face of $[Co(edta)]^-$ in diastereomeric interactions.

Acknowledgment. The support of the National Science Foundation (Grant No. CHE 90-16682) is gratefully acknowledged. Thanks are expressed to a reviewer for bringing attention to the structure of $[Co(en)_3]^{2+}$ and to Dr. Maoyu Shang for help in the preparation of the stereoviews.

Supplementary Material Available: A list of pseudo-first order rate constants for the reduction of $[Co(edta)]^-$ by $[Ru(en)_3]^{2+}$ and tables of fractional coordinates and isotropic displacement parameters for the hydrogen atoms and general atomic displacement parameters and a packing diagram for $[\Lambda\text{-}(+)_{589}\text{-}Co(en)_3][\Delta\text{-}(+)_{546}\text{-}Co(edta)]_2Cl\cdot 10H_2O$ (4 pages). Ordering information is given on any current masthead page.

---

(67) Beattie, J. K. *Acc. Chem. Res.* **1971**, *4*, 253–259.

(68) Geselowitz, D. Ph.D. Dissertation, Stanford University, 1982.

(69) Smolenaers, P. J.; Beattie, J. K.; Hutchinson, N. D. *Inorg. Chem.* **1981**, *20*, 2202–2206.

(70) Newton, M. D. *Chem. Rev.* **1991**, *91*, 767–792.

(71) Duesler, E. N.; Raymond, K. N. *Inorg. Chem.* **1971**, *10*, 1486–1492.

(72) Sarneski, J. E.; Urbach, F. L. *J. Am. Chem. Soc.* **1971**, *93*, 884–888.

(73) Kuroda, R. *Inorg. Chem.* **1991**, *30*, 4954–4959.